Available online at www.sciencedirect.com
SCIENCE DIRECT®
Catalysis Today 102–103 (2005) 189–196
CATALYSIS TODAY
www.elsevier.com/locate/cattod

Characterization and microporosity analysis of mesoporous carbon molecular sieves by nitrogen and organics adsorption

A. Vinu [a,b], Martin Hartmann [a,*]

[a] Department of Chemistry, Chemical Technology, Kaiserslautern University of Technology, P.O. Box 3049, D-67653 Kaiserslautern, Germany
[b] International Center for Young Scientists, National Institute for Materials Science, 1-1 Namiki, Tsukuba 305-0044, Japan

Available online 31 March 2005

Abstract

Novel mesoporous carbon molecular sieves have been prepared from SBA-15 materials as templates at different temperatures. This allows the synthesis of hexagonally arranged mesoporous carbons with pore diameters between 3.0 nm (CMK-3-100) and 6.5 nm (CMK-3-150). CMK-1 and CMK-2 have been synthesized using MCM-48 and SBA-1, respectively, as templates for comparison with the above materials. The structural order and textural properties of all the materials were studied by X-ray diffraction (XRD) and nitrogen adsorption. The microporosity analysis of different mesoporous carbons such as CMK-1, CMK-2, CMK-3, CMK-3-130 and CMK-3-150 has been studied by *n*-heptane and cyclohexane adsorption. It has been found that CMK-2 has a large amount of micropores (upt to 50% of the total pore volume), while the other materials studied possess smaller amounts of micropores. Moreover, it was found that the mechanical stability of CMK-3-100 is high compared to mesoporous SBA-15 silica materials.

Keywords: Mesoporous carbon; CMK-3; Organics adsorption; Mechanical stability; Microporosity

1. Introduction

Porous materials have received much attention in recent years because of their wide range of applications in catalysis, adsorption and sensing [1]. The synthesis of well ordered mesoporous inorganic materials with pore diameters ranging from 2 to 30 nm has opened up a new research field in advanced materials science [2,3]. These materials have been synthesized using either cationic surfactants or neutral non-ionic polymeric surfactants as templates. The resulting materials exhibit well-defined pore structures, a high specific surface area and a large specific pore volume.

Porous carbon materials are used as catalysts, battery electrodes, capacitors, and adsorbents [4]. For some applications, the carbon materials should possess a high mesoporosity allowing the adsorption of molecules and ions that are too large to enter micropores. Recently, Ryoo and co-workers [5–7] prepared ordered mesoporous carbons (CMK-*X*) from mesoporous silica templates such as MCM-48, SBA-1 and SBA-15 using sucrose as the carbon source. Independently and somewhat later, similar approaches were published by Hyeon and co-workers (the materials were designated SNU-*X*) [8]. These novel mesoporous carbon materials are characterized by large specific surface areas, large specific pore volumes and electrical conductivity. Mesoporous carbon materials with regular three-dimensionally arranged pores using AlMCM-48 as the template and employing phenol-formaldehyde resin as the carbon source have been prepared by Lee et al. [9]. It has been reported that these materials show excellent performance as an electrochemical double layer capacitor. Moreover, Yoon et al. [10] synthesized mesoporous carbons from silylated MCM-48 using divinylbenzene as the carbon source. It has been found that the structural integrity and thermal stability of the latter carbon materials are largely improved in comparison to mesoporous carbons prepared with sucrose as the carbon source.

Platinum and palladium supported on the mesoporous carbon CMK-1 has been found to be active in the liquid phase hydrogenation of nitrobenzene, 2-ethylanthraquinone or 4-isobutylacetophenone [11]. Compared with catalysts obtained by supporting precious metals on commercial

* Corresponding author. Tel.: +49 631 205 3559; fax: +49 631 205 4193.
E-mail address: hartmann@chemie.uni-kl.de (M. Hartmann).

0920-5861/$ – see front matter © 2005 Elsevier B.V. All rights reserved.
doi:10.1016/j.cattod.2005.02.028

carbon supports, catalysts based on mesoporous carbons gave better conversion and selectivity at the same metal loading of 5 wt.%. Moreover, ordered mesoporous carbons have demonstrated their potential as catalysts support for O_2 reduction in a fuel cell setup [7,12].

Although the adsorption of organics [13–21] has been thoroughly investigated over mesoporous silica molecular sieves, there is up till now no report on the adsorption of organics on mesoporous carbon molecular sieves. In contrast, the adsorption of organics on activated carbon [22–28], carbon nanotubes [29,30] and nonporous carbon blacks [31–33] has been thoroughly investigated. Bansode et al. [22] have studied the adsorption efficiency of different shell-based granular activated carbons in benzene and chloroform adsorption. Chiang et al. [23] have determined the temperature dependence of the adsorption of volatile organic compounds over different activated carbons. They have also investigated the pore structure of different activated carbons using organic adsorption.

Mechanical stability is an important characteristic of an adsorbent or catalyst for most practical applications. Prior to adsorption and catalytic studies, IR or electric conductivity measurements, the fine powders obtained by hydrothermal synthesis are routinely compacted at high pressure into pellets. Therefore, crushing strength is a critical requirement to conserve the pore volume, surface area and pore diameter of the starting material. Moreover, mechanical stability is an important characteristic with respect to industrial applications where the powders typically obtained by hydrothermal synthesis are subject to a shaping process. Several studies have shown that the mechanical stability of mesoporous silica molecular sieves is very low as compared to zeolite and zeotype materials [33–39]. However, very little attention has been given to the mechanical stability of mesoporous carbon molecular sieves. Yoon et al. [40] have synthesized mesoporous carbon materials (AM48T-C) through a direct template carbonization using as-synthesized MCM-48 template. They have found that AM48T-C possesses higher mechanical and thermal stability as compared to mesoporous silica materials.

Very recently, we have prepared mesoporous carbon materials using SBA-15 materials synthesized at different temperatures [41]. These materials have been employed in the adsorption of horse heart cytochrome c from aqueous solution at different pH. In this study, we have found that the protein adsorption capacity is not linearly increasing with the pore volume of the materials. We surmised that this could be due to the presence of micropores, which are not accessible for the bulky protein molecules.

In the present contribution, we report the preparation and characterization of mesoporous carbon materials with various pore diameters. The microporosity of the different mesoporous carbon molecular sieves was studied by adsorption of organics such as *n*-heptane and cyclohexane. It has been found that CMK-2 possesses a larger amount of micropores as compared to other mesoporous carbon materials. Moreover, the mechanical stability of CMK-3-100 was studied by applying different pelletizing pressures and subsequent characterization by X-ray diffraction (XRD), nitrogen and *n*-heptane adsorption. It has been found that the mechanical stability of CMK-3 is very high compared to the mesoporous silica template SBA-15.

2. Experimental

2.1. Materials

Tetraethylorthosilicate, sucrose and triblock copolymer poly(ethylene glycol)-*block*-poly(propylene glycol)-*block*-poly(ethylene glycol) (Pluronic P123, molecular weight = 5800, $EO_{20}PO_{70}EO_{20}$) were obtained from Aldrich.

2.2. Synthesis of mesoporous CMK-3 carbons with various pore diameters

Mesoporous CMK-3 carbons with different pore diameter were prepared by using different SBA-15-*X* (*X* denotes the synthesis temperature of the silica material) materials as templates and sucrose as the carbon source. The synthesized materials were designated as CMK-3-100, CMK-3-130 and CMK-3-150. In a typical synthesis of mesoporous carbon, 1 g of the mesoporous silica template was added to a solution obtained by dissolving 1.25 g of sucrose and 0.14 g of H_2SO_4 in 5 g of water. The obtained mixture was kept in an oven for 6 h at 100 °C. Subsequently, the oven temperature was raised to 160 °C for another 6 h. In order to obtain fully polymerized and carbonized sucrose inside the pores of the silica template, 0.8 g of sucrose, 0.09 g of H_2SO_4 and 5 g of water were again added to the pretreated sample and the mixture was again subjected to the thermal treatment described above. The template–polymer composites were then pyrolyzed in a nitrogen flow at 877 °C and kept under these conditions for 6 h to carbonize the polymer. The mesoporous carbon was recovered after dissolution of the silica framework in a 5 wt.% solution of hydrofluoric acid by filtration, washed several times with ethanol and dried at 120 °C.

2.3. Synthesis of CMK-1 and CMK-2

CMK-1 and CMK-2 were synthesized by using SBA-1-(48H)[42] and MCM-48, respectively, as template and sucrose as carbon source by an analogous procedure as employed for the synthesis of CMK-3 [6,7].

2.4. Characterization

The SEM images were recorded with a JSM-6500 instrument using an acceleration voltage of 20 kV. The powder X-ray diffraction patterns of mesoporous carbon materials were collected on a Siemens D5005 diffractometer

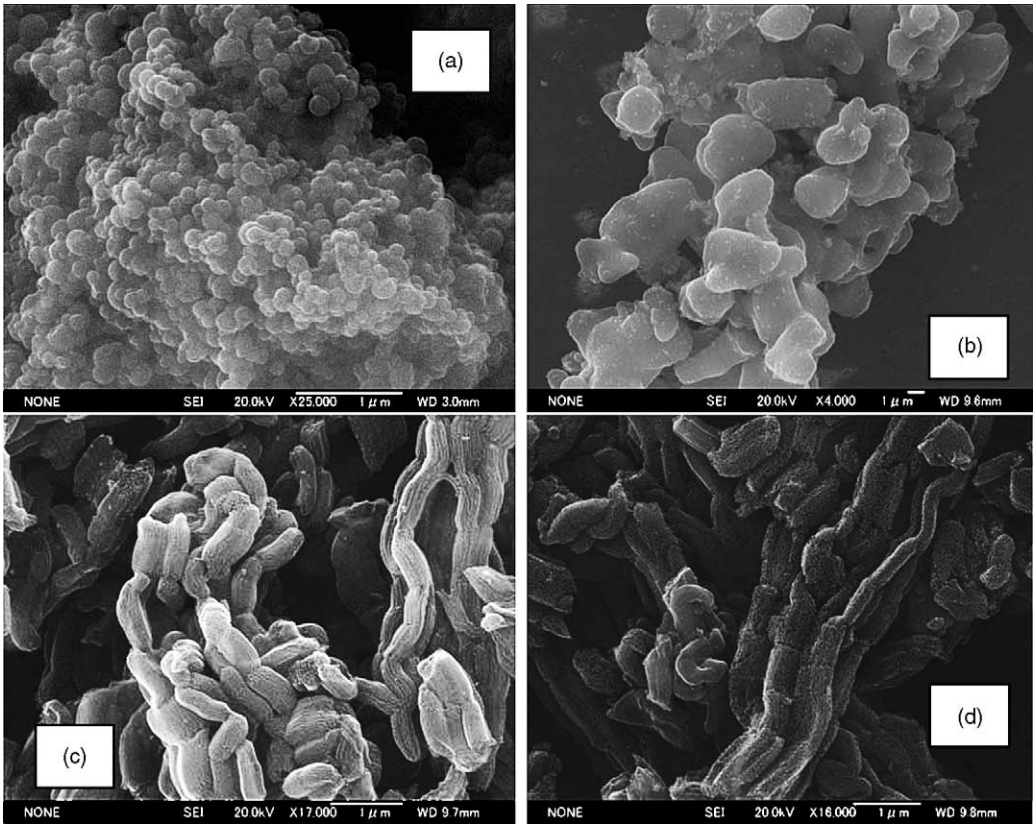

Fig. 1. SEM pictures of: (a) CMK-1; (b) CMK-2; (c) CMK-3-100; and (d) CMK-3-130.

using Cu Kα ($\lambda = 0.154$ nm) radiation. The diffractograms were recorded in the 2θ range of 0.8–10° with a 2θ step size of 0.01° and a step time of 10 s. Nitrogen adsorption and desorption isotherms were measured at 77 K on a Quantachrome Autosorb 1 sorption analyzer. All samples were outgassed for 3 h at 250 °C under vacuum ($p < 10^{-5}$ h Pa) in the degas port of the adsorption analyzer. The specific surface area was calculated using the BET model. The pore size distributions were obtained from the adsorption and desorption branch of the nitrogen isotherms by the Barrett–Joyner–Halenda method and the NLDFT method, respectively.

In order to test the mechanical stability of CMK-3 (i.e. CMK-3-100), the samples were compressed in a steel die of 24 or 12 mm diameter, using a hand-operated press, for 30 min. The five different external pressure applied (0, 217, 590, 738, 1107 MPa) were calculated from the external force applied and the diameter of the die. Subsequently, the obtained disc was crushed and sieved to obtain pellets with a diameter of 0.2–0.35 mm, which were used for all further measurements. The unpressed material was denoted as CMK-3. The other samples were denoted as CMK-3(p), where p specifies the pressure in MPa. Cyclohexane adsorption and *n*-heptane adsorption isotherms at 286 K were recorded using a home-built volumetric adsorption apparatus. Prior to the adsorption experiments, the samples were dehydrated at 200 °C under vacuum ($p < 10^{-6}$ h Pa) for 4 h.

3. Results and discussion

Fig. 1 shows the scanning electron microscopy images of the mesoporous carbons CMK-1, CMK-2, CMK-3-100 and CMK-3-130. It is interesting to note that the materials exhibit different morphologies such as rods (CMK-3), plates (CMK-2) and spheres (CMK-1). Fig. 2 shows the powder X-ray diffraction patterns of CMK-3-100, CMK-3-130 and CMK-3-150. These materials are hexagonally ordered mesostructures as evident from the presence of at least three reflections that can be indexed to the: (1 0 0); (1 1 0) and (2 0 0) reflections of the two-dimensional hexagonal space group *p6mm*. Conse-

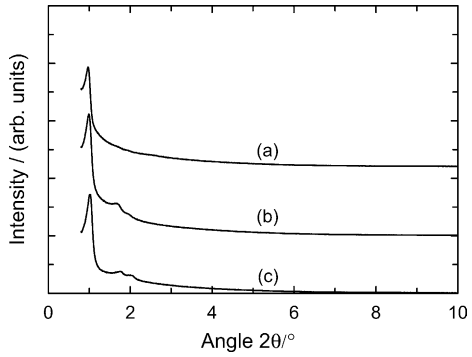

Fig. 2. XRD powder patterns of; (a) CMK-3; (b) CMK-3-130; and (c) CMK-3-150.

Table 1
Textural properties of different mesoporous carbon materials

Sample	d spacing (nm)	A_{BET} ($m^2\ g^{-1}$)	V_p ($cm^3\ g^{-1}$)	$d_{p,BJH}$ (nm)	$d_{p,NLDFT}$ (nm)	Carbon wall thickness, w (nm)
CMK-1	5.14^{d210}	1675	1.05	2.3	–	–
CMK-2	3.51^{d210}	1934	1.17	2.0	–	–
CMK-3-100	8.72	1260	1.10	3.0	3.3	5.4
CMK-3-130	9.05	1250	1.25	4.3	4.3	4.8
CMK-3-150	9.32	1350	1.58	6.5	5.4	3.9

quently, the synthesized materials are a true replica of the parent material SBA-15 [21].The low intensity of the higher order reflections in the case of CMK-3-150 indicates that some structural changes occurred during the silica template removal. This reduced stability is probably a consequence of the changes in the number and size of the carbon rods (formed from the micropores of SBA-15) that connect the carbon rods formed from the main pores of SBA-15. The number of micropores is drastically reduced in the case of SBA-15-150, which is used as template for CMK-3-150 [21]. Moreover, it is interesting to note that the d spacing of the mesoporous carbon synthesized using SBA-15 materials with different pore diameters as templates increases in the following order: CMK-3-150 > CMK-3-130 > CMK-3-100 (Table 1).

Powder X-ray diffraction patterns of the mesoporous carbons CMK-1 and CMK-2 are shown in Fig. 3 in comparison to the silica templates used for their synthesis. CMK-1 exhibits three reflections in the region $2\theta = 2$–3.5° which are indexed to: (1 1 0); (2 1 1) and (2 2 0) reflections of the cubic space group $I4_132$. Higher order reflections are observed in the region $2\theta = 3.5$–6.5 which are a superposition of various reflections that are indexed according to the $I4_132$ space group. The X-ray diffraction pattern of CMK-2 contains three reflections which are indexed to the: (2 0 0); (2 1 0) and (2 1 1) reflections according to the cubic space group *pm*3*n* (Fig. 3). This indicates that the structure of SBA-1-(48H) [42] is retained in the CMK-2 material. However, when SBA-1(0H) is used for the preparation of CMK-2 only a disordered structure is obtained. Therefore, we decided to use SBA-1-(48H) instead of SBA-1(0H) for the preparation of CMK-2 materials in order to get a well-ordered material. The higher structural order of CMK-2 prepared in this way is probably a consequence of the larger pore and cage diameters of SBA-1-(48H) [42].

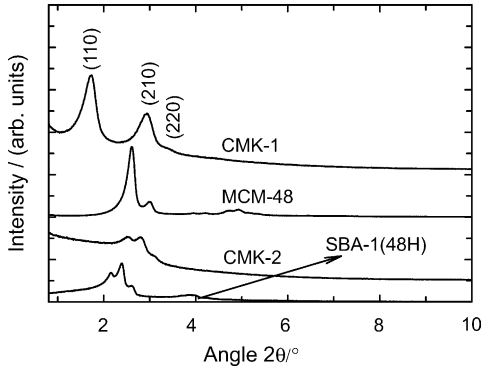

Fig. 3. XRD powder patterns of CMK-1 and CMK-2 and the silica templates used for their synthesis.

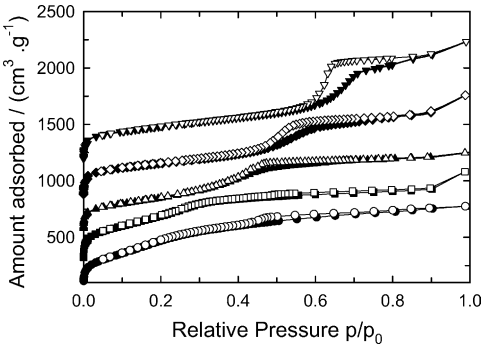

Fig. 4. Nitrogen adsorption isotherms of different mesoporous carbon materials: (●) CMK-1; (■) CMK-2; (▲) CMK-3; (◆) CMK-3-130; and (▼) CMK-3-150. The isotherms are shifted for clarity.

Information on the textural properties of porous solids is typically obtained from low-temperature (77 K) nitrogen adsorption isotherms, which allow calculation of specific surface area, specific pore volume and pore size distribution. Fig. 4 shows the nitrogen adsorption isotherms of CMK-3-130 and CMK-3-150 in comparison to CMK-3-100, CMK-2 and CMK-1. The isotherms of CMK-3-100, CMK-3-130 and CMK-3-150 are of type IV according to the IUPAC classification and exhibit a H1 hysteresis loop. The materials obtained from SBA-15 synthesized at 130 and 150 °C possess pores with diameters of about 4.3 and 6.5 nm (Fig. 5). The specific surface areas and pore volumes of all materials used in the present study are collected in Table 1.

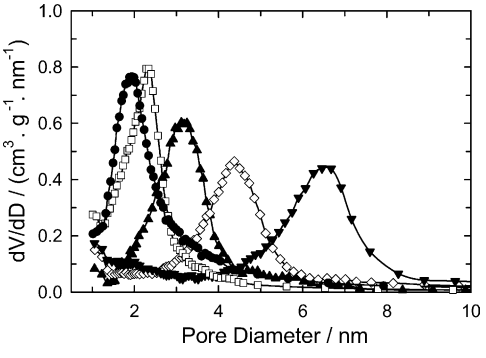

Fig. 5. Pore size distribution of different mesoporous carbon materials: (●) CMK-1; (□) CMK-2; (▲) CMK-3; (◇) CMK-3-130; and (▼) CMK-3-150.

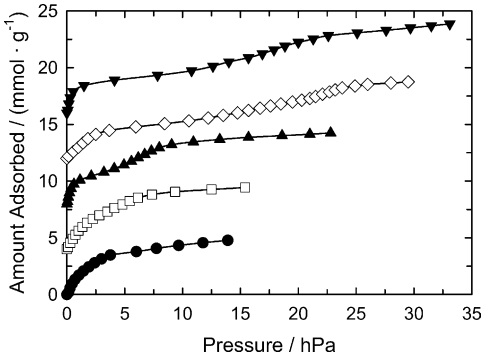

Fig. 6. *n*-Heptane adsorption isotherms at 286 K of different mesoporous carbon materials: (●) CMK-2; (□) CMK-1; (▲) CMK-3; (◇) CMK-3-130; and (▼) CMK-3-150. The isotherms are shifted for clarity.

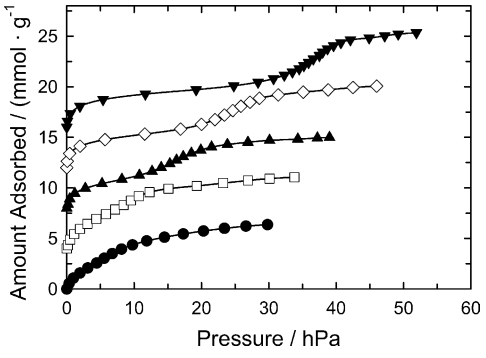

Fig. 7. Cyclohexane adsorption isotherms at 286 K of different mesoporous carbon materials: (●) CMK-2; (□) CMK-1; (▲) CMK-3; (◇) CMK-3-130; and (▼) CMK-3-150. The isotherms are shifted for clarity.

3.1. Microporosity analysis

Although the structure of different mesoporous carbons has been carefully characterized [5–7,41], to the best of our knowledge, there is no report on the microporosity analysis of those materials. To analyze the microporosity of the different mesoporous carbon, the adsorption of organics such as *n*-heptane and cyclohexane has been investigated. The adsorption isotherms of *n*-heptane and cyclohexane at 287 K are shown in Figs. 6 and 7. All adsorption isotherms are of type IV according to the IUPAC classification. The total uptake of organics after the pore condensation are used to calculate the total pore volume (by applying the Gurvich rule) accessible to large molecules such as *n*-heptane and cyclohexane. Pore volumes were calculated from the amount adsorbed assuming that the density of the adsorbed phase is equal to the density of bulk liquid at adsorption temperature. The total pore volume accessible to large molecules such as *n*-heptane and cyclohexane is calculated from the total uptake of organics after the pore condensation step is complete.

The pore volumes calculated from *n*-heptane and cyclohexane adsorption isotherms are summarized in Table 2. The pore volumes calculated from the uptake of *n*-heptane and cyclohexane are significantly lower than the pore volumes determined from nitrogen adsorption. The amount of *n*-heptane and cyclohexane adsorbed is decreasing in the following order: CMK-2 < CMK-3-150 < CMK-3 < CMK-1 < CMK-3-130. In the previous studies on MCM-41and MCM-48, it is also found that the pore volumes determined by adsorption of subcritical organic vapors are systematically lower (10–20%) than the ones calculated from nitrogen data [19]. This is mainly ascribed to the uncertainty of the density of the adsorbed phase, which is taken as the density of bulk liquid at the adsorption temperature (Gurvich rule). In our case, the difference between the pore volume derived from nitrogen adsorption and organics adsorption is large indicating the presence of a substantial amount of micropores in the mesoporous carbon materials. This is further substantiated by the micropore volume calculated using the α_s-method (Table 2). Although somewhat lower, the micropore volume derived from the latter method follows a similar trend. Therefore, we have to assume that mesoporous carbon materials in particular those prepared from sucrose as carbon source contain a significant amount of micropores. CMK-2 possesses a larger amount of micropores compared to other mesoporous carbon materials. This could be due to the small interconnectivity between the main pore channels of the SBA-1 molecular sieves used as template. Thus, some sucrose molecules partially enter the interconnecting pore and some structural disorder results. This is in line with our XRD results exhibiting some structural disorder of these materials. Among the mesoporous carbons prepared by using SBA-15-*X* as template, CMK-3-150 has the highest amount of micropores. These micropores either originate from the incomplete polymerization of sucrose molecules inside the mesopores of the template or from the rupture of carbon–carbon bonds during pyrolysis or from the structural changes occurring during the template dissolution using hydrofluoric acid. It should be

Table 2
Comparison of the pore volume data obtained from nitrogen and organic adsorption isotherms

Sample	$V_p(N_2)$ (cm^3 g^{-1})	n_{ads}(*n*-hp) (mmol g^{-1})	V_p(*n*-hp) (cm^3 g^{-1})	n_{ads}(CHx) (mmol g^{-1})	V_p(CHx) (cm^3 g^{-1})	V_{micro} (cm^3 g^{-1})
CMK-1	1.04	5.05	0.73	5.9	0.75	0.08
CMK-2	1.17	4.44	0.59	4.6	0.61	0.24
CMK-3-100	1.10	5.20	0.76	6.0	0.77	0.12
CMK-3-130	1.25	6.20	0.90	7.2	0.92	0.16
CMK-3-150	1.58	7.07	1.03	8.6	1.10	0.25

The micropore volume V_{micro} was determined by using the α_s-method.

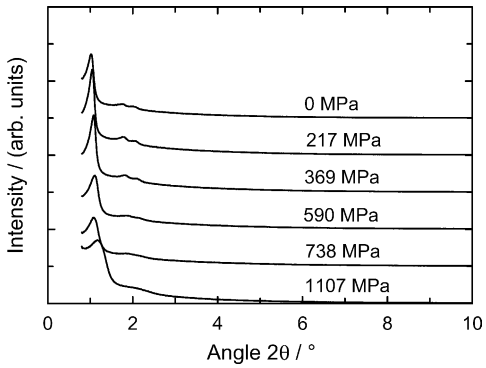

Fig. 8. XRD powder patterns of compressed CMK-3 materials: (a) CMK-3 (0 MPa); (b) CMK-3 (217 MPa); (c) CMK-3 (369 MPa); (d) CMK-3 (590 MPa); (e) CMK-3 (738 MPa); and (f) CMK-3 (1107 MPa).

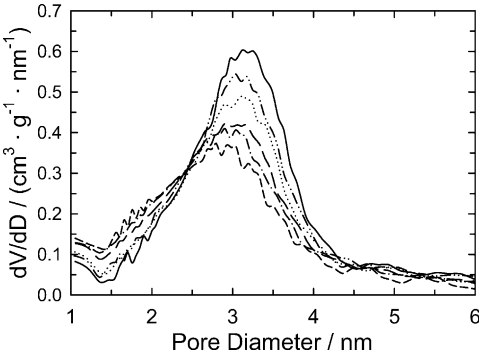

Fig. 10. Pore size distribution of compressed CMK-3 materials: (-) CMK-3; (-·-·-) CMK-3 (217 MPa); (· · ·) CMK-3 (369 MPa); (- - -) CMK-3 (590 MPa); (-·-) CMK-3 (738 MPa); and (— —) CMK-3 (1107 MPa).

noted that mesoporous silica SBA-15 also exhibits a large discrepancy (up to 50%) between the pore volume determined by nitrogen adsorption and organics adsorption [21], which is ascribed to the presence of (ultra)micropores [43,44]. However, from the above results, it has to be concluded that CMK-3-100, CMK-3-130 and CMK-3-150 have fewer micropores compared to the corresponding SBA-15 template.

3.2. Mechanical stability

Fig. 8 exhibits the powder X-ray diffraction patterns of compressed CMK-3(p) (p denotes the pelletizing pressure) samples in comparison to the parent material CMK-3. The quality of XRD patterns is not changing with increasing pelletizing pressure up to 369 MPa (369 N mm^{-2}). From a pressure of 590 MPa onwards, the diffraction peaks broaden considerably. Moreover, it has to be noted that the unit cell parameter decreases with increasing pelletizing pressure. This might suggest that grains containing larger unit cells (i.e. larger pore diameter) are preferentially crushed, while grains containing materials with smaller unit cells are more stable against application of an external force. Moreover, the increased line broadening indicates that the average size of the stable grains is reduced.

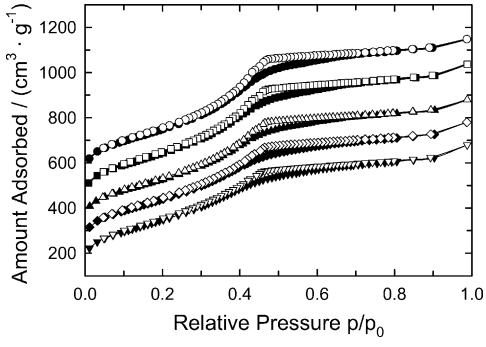

Fig. 9. Nitrogen adsorption isotherms of compressed CMK-3 materials: (●) CMK-3 (217 MPa); (■) CMK-3 (369 MPa); (▲) CMK-3 (590 MPa); (◆) CMK-3 (738 MPa); and (▼) CMK-3 (1107 MPa). The isotherms are shifted for clarity.

The nitrogen adsorption and desorption isotherms of the compressed CMK-3 samples are shown in Fig. 9 and the textural parameters are collected in Table 3. With increasing pelletizing pressure, the specific pore volume decreases slightly, while the mean pore diameter calculated from the adsorption branch of the nitrogen isotherms using the BJH model and the specific surface area are virtually not affected. However, the pore size distribution obtained from the desorption branch of the isotherm is broadened to the low pore diameter side, which indicates some pore deformation upon compression and results in a decrease of the mean pore diameter (Table 3 and Fig. 10). The specific pore volume is reduced from 1.1 to 0.91 cm^3 g^{-1} with increasing pelletizing pressure upto 1107 MPa. The reduction in the pore volume of CMK-3(1107) is only 17.3% compared to the uncompressed CMK-3 materials. However, only a 3.6% reduction of the pore volume is observed for the materials pressed at 217 MPa as compared to the parent material. It has been reported that for high quality MCM-41 and MCM-48, the specific pore volume decreases by 20% of its original value upon compression by 260 MPa [19] while for SBA-15 the

Table 3
Textural properties of the pressed CMK-3 materials

Catalyst (MPa)	Unit cell parameter (nm)	A_{BET} (m^2 g^{-1})	V_p (cm^3 g^{-1})	$d_{ads,BJH}$ (nm)	$d_{des,BJH}$ (nm)
CMK-3 (217)	9.86	1230	1.06	3.3	3.3
CMK-3 (369)	9.52	1176	0.98	3.3	3.2
CMK-3 (590)	9.35	1219	0.97	3.3	3.0
CMK-3 (738)	9.48	1251	0.96	3.4	2.9
CMK-3 (1107)	8.74	1247	0.91	3.3	3.0

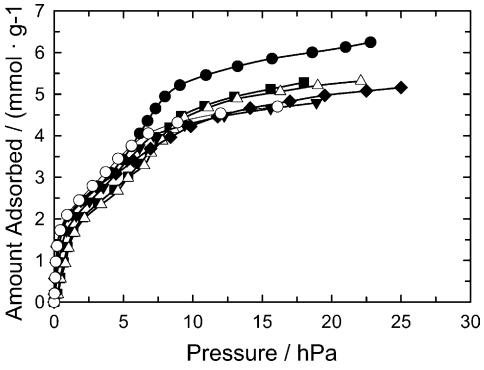

Fig. 11. *n*-Heptane adsorption isotherms at 286 K of compressed CMK-3 materials: (●) CMK-3; (■) CMK-3 (217 MPa); (△) CMK-3 (369 MPa); (◆) CMK-3 (590 MPa); (▼) CMK-3 (738 MPa); and (○) CMK-3 (1107 MPa).

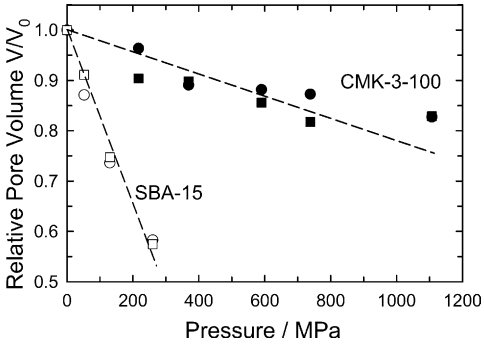

Fig. 12. Comparison of the relative pore volume of SBA-15 (open symbol) and CMK-3 (closed symbol) from (●) nitrogen adsorption isotherm and (■) *n*-heptane adsorption isotherm.

pore volume is diminished by about 40%. Moreover, the mesoporous silica materials such as MCM-41, SBA-15 and MCM-48 are not mechanically stable above a pelletizing pressure of 500 MPa [19,21] These results indicate that the carbon mesoporous molecular sieve CMK-3 is mechanically more stable than the corresponding mesoporous silica molecular sieves.

In Fig. 11, the adsorption isotherms of *n*-heptane at 286 K over the compressed CMK-3(p) materials are depicted in comparison to the unpressed parent material CMK-3. The amount of *n*-heptane adsorbed decreases with increasing pelletizing pressure. However, the difference is small when compared with compressed mesoporous silica materials. The pore volumes calculated from the organic adsorption isotherm are summarized in Table 4. The pore volume V_p(*n*-hp) of the compressed materials decreases only from 0.76 to 0.63 $cm^3\ g^{-1}$ with increasing pelletizing pressure up to 1107 MPa. It is interesting to note that the pore volumes calculated from *n*-heptane adsorption on CMK-3 even after compression at 1107 MPa is only 17.1% lower than that of the parent material CMK-3. It has been reported that among the mesoporous silicas, SBA-1 is the material with the highest mechanical stability [42,45]. Upon compression with 217 MPa, the pore volume of SBA-1 calculated from *n*-heptane adsorption already declines by 12.5%. After compression of SBA-15 with 260 MPa, a more than 40% reduction in the pore volume calculated from *n*-heptane adsorption was observed [21]. In contrast, the pore volume of CMK-3 is only reduced by 9.7% after compression with 217 MPa.

Table 4
Comparison of the pore volume data obtained from nitrogen and organic adsorption isotherm of compressed mesoporous carbon materials

Sample (MPa)	$V_p(N_2)$ ($cm^3\ g^{-1}$)	n_{ads}(*n*-hp) (mmol g^{-1})	V_p(*n*-hp) ($cm^3\ g^{-1}$)
CMK-3 (0)	1.1	5.20	0.76
CMK-3 (217)	1.06	4.70	0.68
CMK-3 (369)	0.98	4.67	0.68
CMK-3 (590)	0.97	4.45	0.65
CMK-3 (738)	0.96	4.25	0.62
CMK-3 (1107)	0.91	4.31	0.63

The relative pore volume V/V_0 (V_0 is the pore volume of the unpressed parent material) calculated from both nitrogen and *n*-heptane adsorption for unpressed and pressed materials is a good measure for the mechanical stability of porous materials (Fig. 12). The reduction in the relative pore volume is very small even for the material compressed at 1107 MPa. Moreover, the decline in the relative pore volume is smaller for CMK-3 compared to other hexagonal phases such as MCM-41, MCM-48 and SBA-15 [19,21]. This is not only due to the higher wall thickness of CMK-3 material as compared to mesoporous silica materials (5.4 nm versus 3 nm) but more correctly due to the higher ratio between wall thickness and pore diameter (w/d_p) [45]. For CMK-3-100, the ratio is 1.8 while it only amounts to 0.18 for the SBA-15 parent material. From theoretical consideration it is therefore expected that the mechanical stability of CMK-3 is significant higher as compared to SBA-15, which is indeed confirmed in the present study.

4. Conclusions

Novel mesoporous carbon molecular sieves have been prepared from SBA-15 materials as templates at different temperatures. This allows the synthesis of hexagonally arranged mesoporous carbons with pore diameters between 3.0 nm (CMK-3) and 6.5 nm (CMK-3-150). CMK-1 and CMK-2 have also been synthesized for comparison with the above materials. The structural order and textural properties of all the materials were studied by XRD, N_2 adsorption and organics adsorption The microporosity analysis of different mesoporous carbons such as CMK-1, CMK-2, CMK-3, CMK-3-130 and CMK-3-150 by *n*-heptane and cyclohexane adsorption has shown that CMK-2 and CMK-3-150 have a larger amount of micropores as compared to the other materials under study. This is probably due to the higher structural disorder of CMK-2 and CMK-3-150. Moreover, it has also been found that the mechanical stability of CMK-3

is significantly higher as compared to mesoporous silica materials such as SBA-15.

Acknowledgments

Financial support of this work by Deutsche Forschungsgemeinschaft (Ha2527/4) and Fonds der Chemischen Industrie is gratefully acknowledged.

References

[1] (a) F. Schüth, W. Schmidt, Adv. Mater. 14 (2002) 629;
(b) J.Y. Ying, C.P. Mehnert, M.S. Wong, Angew. Chem. Int. Ed. Engl. 38 (1999) 57.
[2] (a) J.S. Beck, J.C. Vartuli, W.J. Roth, M.E. Leonowicz, C.T. Kresge, K.D. Schmitt, C.T.W. Chu, D.H. Olson, E.W. Sheppard, S.B. McCullan, J.B. Higgins, J.L. Schlenker, J. Am. Chem. Soc. 114 (1992) 10834;
(b) C.T. Kresge, M.E. Leonowicz, W.J. Roth, J.C. Vartuli, J.S. Beck, Nature 359 (1992) 710.
[3] (a) D. Zhao, Q. Huo, J. Feng, B.F. Chmelka, G.D. Stucky, J. Am. Chem. Soc. 120 (1998) 6024;
(b) D. Zhao, J. Feng, Q. Huo, N. Melosh, G.H. Fredrickson, B.F. Chmelka, G.D. Stucky, Science 279 (1998) 548.
[4] K. Lu, D.D.L. Chung, Carbon 35 (1997) 427.
[5] (a) R. Ryoo, S.H. Joo, S. Jun, J. Phys. Chem. B 103 (1999) 7743;
(b) R. Ryoo, S.H. Joo, M. Kruk, M. Jaroniec, Adv. Mater. 13 (2001) 677.
[6] S. Jun, S.H. Joo, R. Ryoo, M. Kruk, M. Jaroniec, Z. Liu, T. Ohsuna, O. Terasaki, J. Am. Chem. Soc. 122 (2000) 10712.
[7] S.H. Joo, S.J. Choi, I. Oh, J. Kwak, Z. Liu, O. Terasaki, R. Ryoo, Nature 412 (2001) 169.
[8] For a recent review see: J. Lee, S. Han, T. Hyeon, J. Mater. Chem. 14 (2004) 478.
[9] J. Lee, S. Yoon, T. Hyeon, S.M. Oh, K.B. Kim, Chem. Commun. (1999) 2177.
[10] S.B. Yoon, J.Y. Kim, J.-S. Yu, Chem. Commun. (2001) 559.
[11] W.S. Ahn, K.I. Min, Y.M. Yung, H.-K. Rhee, S.H. Joo, R. Ryoo, Stud. Surf. Sci. Catal. 135 (2001) 313.
[12] J.-S. Yu, S. Kang, S.B. Yoon, G. Chai, J. Am. Chem. Soc. 124 (2002) 9382.
[13] C. Nguyen, C.G. Sonwane, S.K. Bhatia, D.D. Do, Langmuir 14 (1998) 4950.
[14] J. Jänichen, H. Stach, M. Busio, J.H.M.C. Van Wolput, Thermochim. Acta 312 (1998) 33.
[15] T. Boger, R. Roesky, R. Glaeser, S. Ernst, G. Eigenberger, J. Weitkamp, J. Microporous Mater. 8 (1997) 79.
[16] J. Rathousky, A. Zukal, O. Franke, G.J. Schulz-Ekloff, J. Chem. Soc., Faraday Trans. 91 (1995) 937.
[17] O. Franke, G.J. Schulz-Ekloff, J. Rathousky, J. Starech, A. Zukal, J. Chem. Soc., Chem. Commun. (1993) 724.
[18] C.-Y. Chen, S.Q. Xiao, M.E. Davis, Microporous Mater. 4 (1995) 1.
[19] M. Hartmann, C. Bischof, J. Phys. Chem. B 103 (1999) 16230.
[20] M. Hartmann, C. Bischof, Prepr. - Am. Chem. Soc., Div. Pet. Chem. 46 (2001) 23.
[21] M. Hartmann, A. Vinu, Langmuir 18 (2002) 8010.
[22] R.R. Bansode, J.N. Losso, W.E. Marshall, P.M. Rao, R.J. Portier, Bioresour. Technol. 90 (2003) 175.
[23] Y.-C. Chiang, P.-C. Chiang, C.-P. Huang, Carbon 59 (2001) 523.
[24] L.-Q. Li, J.R. Hangs, D.S. Wolf, Ziran Kexueban 30 (2003) 47.
[25] D.-F. Li, H. Zeng, J.-Q. Wang, Y. Zhang, Shiyou Huagong 30 (2001) 677.
[26] M.L. Gubkina, N.S. Polyakov, G.A. Petukhova, O.V. Kalmykova, E.A. Ustinov, Russ. Chem. Bull. 50 (2001) 595.
[27] Q.-Y. Chen, W.H. Yuan, J.-Y. Guan, Ziran Kexueban 28 (2000) 117.
[28] H.L. Chiang, C.P. Huang, P.C. Chiang, Chemosphere 46 (2002) 143.
[29] Z. Mao, S.B. Sinnott, J. Phys. Chem. B 105 (2001) 6916.
[30] G.U. Sumanasekera, B.K. Pradhan, H.E. Romero, K.W. Adu, P.C. Eklund, Phys. Rev. Lett. 89 (2002) 166801.
[31] A. Ciembroniewicz, J. Klinik, A. Korta, A. Nodzenski, K. Rewilak, Gornictwo 85 (1977) 9.
[32] T.V. Baikova, M.L. Gubkina, K.M. Nikolaev, N.S. Polyakov, Seriya Khimicheskaya 8 (1993) 1381.
[33] V.Y. Gusev, X. Feng, Z. Bu, G.L. Haller, J.A. O'Brien, J. Phys. Chem. B 100 (1996) 1985.
[34] K.A. Koyano, T. Tatsumi, J. Phys. Chem. B 101 (1997) 9436.
[35] T. Tatsumi, K.A. Koyano, Y. Tanaka, S. Nakata, J. Porous Mater. 6 (1999) 13.
[36] D. Desplantier-Giscard, O. Collart, A. Galarneau, P. Van der Voort, F. Di Renzo, F. Fajula, Stud. Surf. Sci. Catal. 129 (2000) 665.
[37] T. Ishikawa, M. Matsuda, A. Vasukawa, K. Kandori, S. Inagaki, T. Fukushima, S.J. Konda, J. Chem. Soc., Faraday Trans. 92 (1996) 1985.
[38] M.-A. Springuel-Huet, J.-L. Bonardet, A. Gédéon, Y. Yue, V.N. Rommannikov, J. Fraissard, Microporous Mesoporous Mater. 44–45 (2001) 775.
[39] A. Galarneau, D. Desplantier-Giscard, F. Di Renzo, F. Fajula, Catal. Today 68 (2001) 191.
[40] S.B. Yoon, J.Y. Kim, J.-S. Yu, Chem. Commun. (2002) 1536.
[41] A. Vinu, C. Streb, V. Murugesan, M. Hartmann, J. Phys. Chem. B 107 (2003) 8297.
[42] A. Vinu, V. Murugesan, M. Hartmann, Chem. Mater. 15 (2003) 1385.
[43] P. Van der Voort, P.I. Ravikovitch, K.P. de Jong, M. Mejelloun, E. van Bavel, A.H. Janssen, A.V. Neimark, B.M. Weckhuysen, E.F. Vasant, J. Phys. Chem. B 106 (2002) 5873.
[44] A. Galarneau, H. Cambon, F. Di Renzo, R. Ryoo, M. Choi, F. Fajula, New J. Chem. 27 (2003) 73.
[45] M. Hartmann, A. Vinu, Stud. Surf. Sci. Catal. 146 (2003) 285.